Nanotechnology Perceptions
ISSN 1660-6795
www.nano-ntp.com

Influence Of MIG Welding Arc Modes On Wire Arc Additive Manufacturing Of SS 316L

Karpagaraj Anbalagan

Department of Mechanical Engineering, National Institute of Technology Puducherry, Karaikal - 609609, India.
** karpagaraj@nitpy.ac.in*

Gas Metal Arc Welding (GMAW) with different arc modes like Direct Current (DC) and Direct Current Pulsed (DCP) was used to melt stainless steel 316L (SS 316L) wire for thin-wall fabrication. Mechanical properties, including tensile fractography, microhardness, and hot corrosion resistance, are assessed and compared with SS 316L base metal. Bead on Plate (BoP) trials were conducted by varying the process parameters for studying the optimal welding parameter from GMAW. The SS 316L material fabricated using the Wire Arc Additive Manufacturing (WAAM) process exhibits a fine equiaxed grain structure with minimal porosity. The microhardness analysis demonstrates that the DC pulsed mode material has the highest value at approximately 259.16 Hv. The tensile strength for the DCP walls was recorded as 603 MPa, compared to Base (662 MPa) and DC (542 MPa), respectively. The fracture analysis showed that all specimens have the ductile fracture mode under tensile load. The base material proves the most negligible mass changes in the hot corrosion test. When exposed to different salt environments, 5% V_2O_5 showed the highest corrosive environment in all samples. The resistance of WAAM-deposited stainless steel 316L meets the requirements for various industrial applications.

Keyword: - Stainless Steel 316l, Waam, Mig Welding, Tensile Test, Hot Corrosion.

1 INTRODUCTION

Ferrous alloys satisfy the needs of modern engineering life. Preferably, Stainless steel is used in most domestic and industrial applications. Stainless steel 316L is widely used in power plants, medical and domestic applications [1-2]. The need for these steel applications is increasing day by day. Various manufacturing methods are implemented at the global level to meet the demand. Rane et al. (2018) investigated the rapid production of hollow SS316 profiles by extrusion-based additive manufacturing [3]. It was found that the extrusion-based additive manufacturing process has produced complex-shaped parts with a near theoretical density of ~90% and a uniform microstructure. The effect of the incomplete debonding stage was reflected in sintered density and chemical composition. The control over residual carbon in sintered parts via prolonged debonding may reduce the formation of chromium carbides and prevent undesirable grain growth. Zhong [4] studied the sub-grain structure in SS316L prepared by Selective Laser Melting (SLM) and Electron Beam Melting (EBM). It was found that SLM has better strength while EBM has better ductility. Balit et al. [5] studied the

relationship between the parameters of a Directed Energy Deposition (DED) process. The result indicated that grains grown by epitaxy from the substrate had an elongated shape. Also, chemical segregation occurs with a loss of Iron and a gain of Molybdenum and Chromium.

Karpagaraj et al. (2020) investigated a review on the suitability of Wire Arc Additive Manufacturing (WAAM) for stainless steel 316. WAAM is a process by melting the metal wire by the use of heat any welding techniques like Laser beam, Electron beam and arc welding process. The wire will be supplied from the wire spool as external or by internal mechanism. The metal deposition will be a layer by layer to make the WAAM process. It was reported that new technologies are developed for manufacturing and processing steel and must be updated to meet the demand. But the manufacturing methods mentioned above are too costly. So, researchers focus on low-cost, less-aid equipment to produce the SS316L components [6]. One recent manufacturing method is Wire Arc Additive Manufacturing (WAAM). Rodrigues et al. Reported that complex and different types of parts can be successfully fabricated by the WAAM [7]. The history of heating and cooling cycles was found to be essential for the stress and phase segregation in WAAM walls. The microhardness of the components is modified as per the heat treatment. Chen et al. (2017) studied additive manufacturing of SS316L using Gas Metal Arc Welding (GMAW) [8]. It was highlighted that increasing the heat treatment temperature and time helped the SS 316 to improve the corrosion properties. Heat treatment after 1000℃ effectively increases the amount of σ phase in steel with spheroidization of the remaining δ phase. Also, the σ phase completely dissolves in γ matrix if the heat treatment is done by 1100℃ and 1200℃ for one hour. Wanget et al. (2019) investigated the Wire Arc Additive Manufacturing (WAAM) of SS316L by varying the parameters such as speed pulse and arc. It was found that significantly efficient and structurally sound outcomes are achieved by optimizing the speed pulse and arc. The strength of the samples made by horizontal direction has shown more than the base metal [9].

Chen et al. (2021) investigated the dynamic mechanical properties of 316L stainless steel fabricated by an additive manufacturing process. As built, Cold Metal Transfer (CMT) 316L samples consists of coarse columnar grain allied with the placing direction. Also, minute areas of dispersed ferrite (less than 5%) in dendrite were formed in the same order. Twinning is the primary deformation mechanism for 316L component fabricated by CMT under dynamic compression. Related to wrought materials, dynamic yield strength and flow stress for walls made with CMT are higher at minor strains due to the particular cellar structure in the matrix [10]. Vishnukumar et al. studied the effect of post-processing of SS316L walls build by Gas Metal Arc Welding (GMAW). It was found that post-heat treatment can enhance corrosion resistance. The corrosion rate ranged between 0.5 and 3.0 mils per year (mpy), suggesting that SS316L is an inexpensive material with compact passive film formation [11]. However, the effect of welding process parameters with MIG welding modes is not yet fully revealed for the SS316L walls. So, making and building the WAAM using direct and pulsed currents may help the engineers. Cunningham et al. investigated the role of heat input and inter-pass temperature on 316LSi deposited by the WAAM process. These parameters have a significant role in the phase change morphology. Also, the heat input contributes to modifying the Young's modulus of the fabricated wall. Heat input and inter-pass cooling will reflect the part functionality [12].

Based on the literature, it was found that welding modes and their effect on the mechanical and hot corrosion behaviors need more focus. So, in this study, modes like DC and

DCP are chosen for building the walls using the MIG welding process. The results are summarized in the articles.

2 EXPERIMENTAL WORK

The filler material selected for this research is stainless steel 316L. The filler material composition is displayed in Table 1. A Welbee 400P low spatter with an automation controller is the welding machine used for building the wall. The welding power source has three modes: Direct Current (DC) and Direct Current Pulse (DCP). The complete setup with the necessary arrangement is shown in Figure 1.

Table 1 Stainless steel 316L filler material composition

Element	C	Cr	Mn	Mo	Ni	N	P	Si	S	Iron (Fe)
Weight (%)	0.03	16.50 - 18.50	2.00	2.00 - 2.50	10.00 - 3.00	0.10	0.045	1.00	0.015	Balance

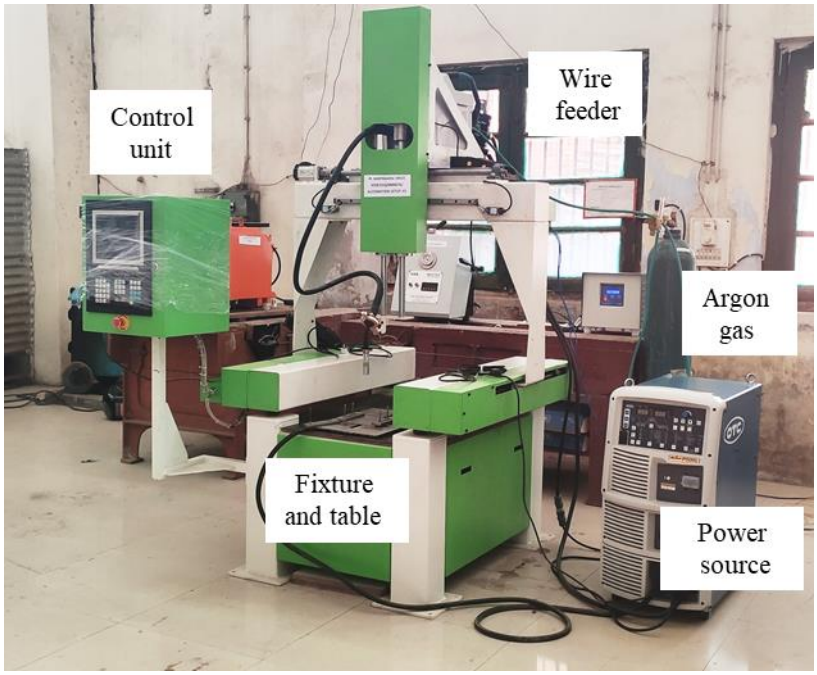

Figure 1. Experimental setup used for the wall-building

Initially, few trials are conducted, and the feasibility of selecting the optimal parameters is done from the preliminary studies. Also, the suggestions and remarks from the previous studies are used here for the same purpose. The samples are machined using the milling machine. Using the wire cut EDM, tensile test, corrosion, hot corrosion, and metallurgical samples are

prepared. For the tensile test, ASTM E8M-04 is followed. The 1 mm/min strain rate is applied to the samples for the tensile test. The fracture portions are further studied with SEM mode. Chemical etching is used on the samples to identify the microstructure present at the walls.

Hot corrosion test was performed in the tubular furnace on the SS316L, DC and DCP at 900°C exposed to different salt mixtures (salt mixture 1 (70% Na2SO4+ 25% NaCl +5% V2O5), salt mixture 2 (75% Na2SO4 + 23% NaCl + 3% V2O5), and salt mixture 3 (75% Na2SO4 + 25% NaCl)). (Nano Tech, Chennai-India). Wire-cut EDM was used to extract the specimen, with dimensions of 20 ×15×5mm. All of the specimen's faces were mirror-polished, cleaned, and placed in the furnace using the alumina crucible. The weight of the sample is noted at the initial condition and operation temperature (900°C) with one-hour intervals. Around 50 cycles are performed for 50 hours to identify the hot corrosion effect on the samples.

3 RESULTS AND DISCUSSION

3.1 Pre-processing

The selected parameters and the modes are listed in Table 2. Auto synchronous mode is set for more optimization in wall building (Figure 2). The layer profile is identified after each deposition. Later, the walls are machined using the milling machine to remove the bur, scales, and layer profiles (Fig 2.).

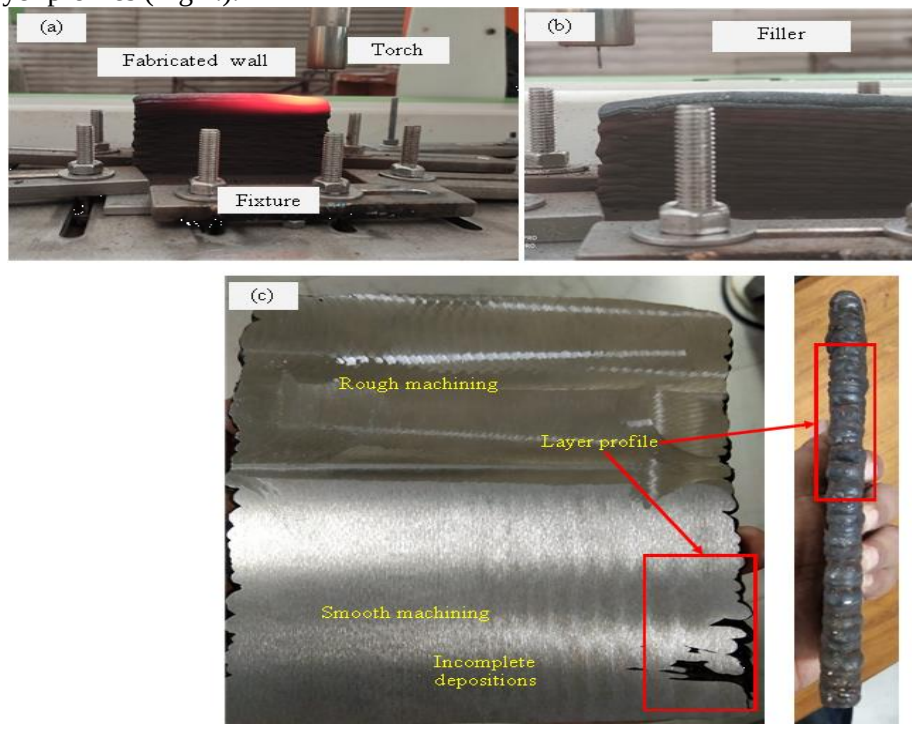

Figure 2. Wall (a) As-built condition, (b) After cooling, and (c) After the milling process

Table 2. The welding parameters and their modes

S.no	Welding mode	Welding current (A)	Welding speed (mm/min)	Heat input (kJ/mm)	Remark
1	DC	120	250	530 $X10^{-3}$	Bead with a smooth profile
2	DCP	90 (I_{avg})	250	387 $X\ 10^{-3}$	Bead with a few spatters at the initial

The side view shows that walls are not getting more distortion due to the heat input and cooling rate. In the milling process, one rough milling is initially performed, and then fine milling is done. From Figure 3, the proper area is identified after the milling process. Some incomplete deposition is placed on the bottom side of the wall. The walls are built and checked for defects. Defects such as delamination, voids, and porosities are not found in the samples after the machining. [13-15]

3.2 Tensile test and fractography

The build sample's tensile test uses Dc and DCP modes. Since the layer deposition is free from the defects, it is unique to check the strength and elongation by conducting it through the tensile test. Tensile test samples are extracted as per the ASTM standards. The base metal of SS316L showed 507 MPa as a maximum, and the DC mode sample showed a minimum of 423.46 MPa. The strength of the DCP mode sample lies in between both. The difference is 10% for DCP to base metal, but for DC to base metal, it is 16.5%. In elongation, DCP showed 55.4%, whereas base metal showed an elongation of 49.5%. The fine micro structure present at the base metal supported optimal yield with higher strength, as the evident from the plot. But for the WAAM samples the weld thermal cycle has modified the micro structure and grain coarsening caused the more elongation with nominal strength reduction. As listed in the literatures faster the cooling rate by laser welding and slower cooling is achieved by the GTAW process. Due this different cooling rate the finer structures are produced with laser welding and coarse structure are produced by GTAW process. These different in cooling rates are leads to the elongation and toughness of the samples also in hardness variations too [16-18]. Due to these reasons the performance of the WAAM samples are deviated little bit from the base substrate. For further analysis, the fractured specimens are engaged with SEM. [11-12]

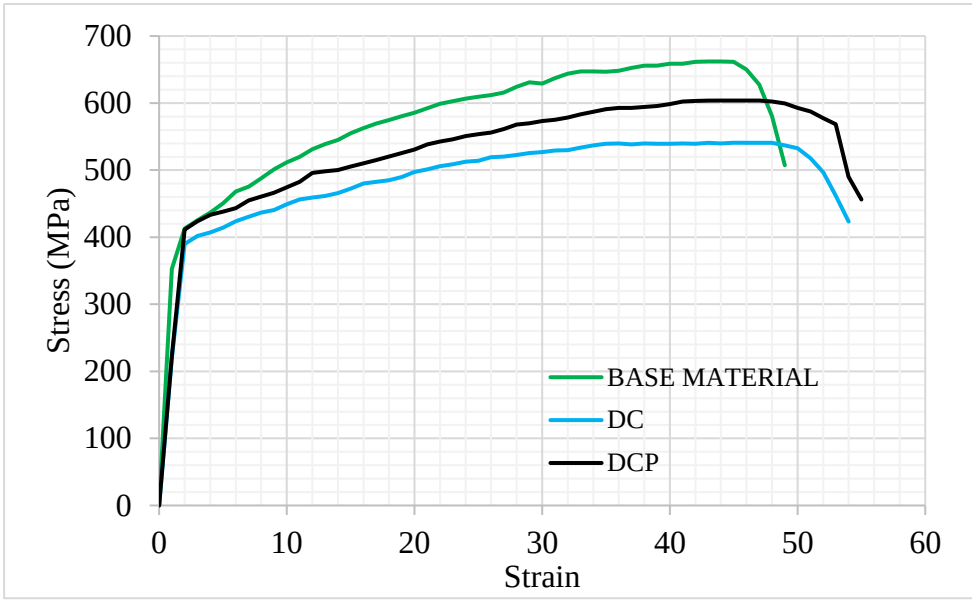

Figure 3. Stress-strain curve for Base, DC, and DCP

The fractography shows dimples in base materials, but fine dimples are found in the DC sample. Dimples with secondary cracks are present in the DCP sample. But in base material, macro voids are present. Similar voids are located in the DC samples, but the size is smaller than the voids present in the base material (fig. 4). The presence of the fine dimples is evident for higher elongation achieved by the DC sample. Also, the secondary cracks are the reason for the increase in the strength of the DCP sample.

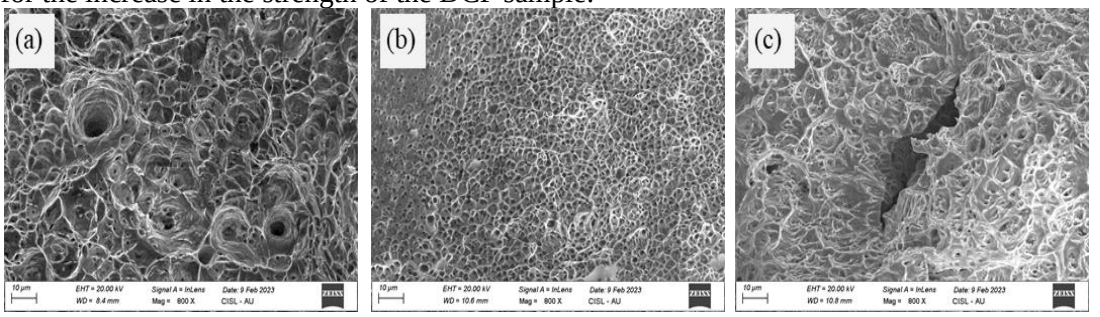

Figure 4. Fractography for Base, DC, and DCP

3.3 Microhardness

The microhardness measurement for the Base wall build with two different conditions is performed. The indentations are taken three times, and the average value is taken. The DC mode (206.86 HV 0.5) walls showed nearly four counts more as compared with the Base. Also, the DCP mode (213 HV 0.5) walls are shown eleven counts higher than the Base. The base metal showed more elongation, which proved against their microhardness. The effect of MIG welding, cooling rate, and the segregation of alloying elements is the reason for increasing the hardness in walls made with DC and DCP modes. [7]

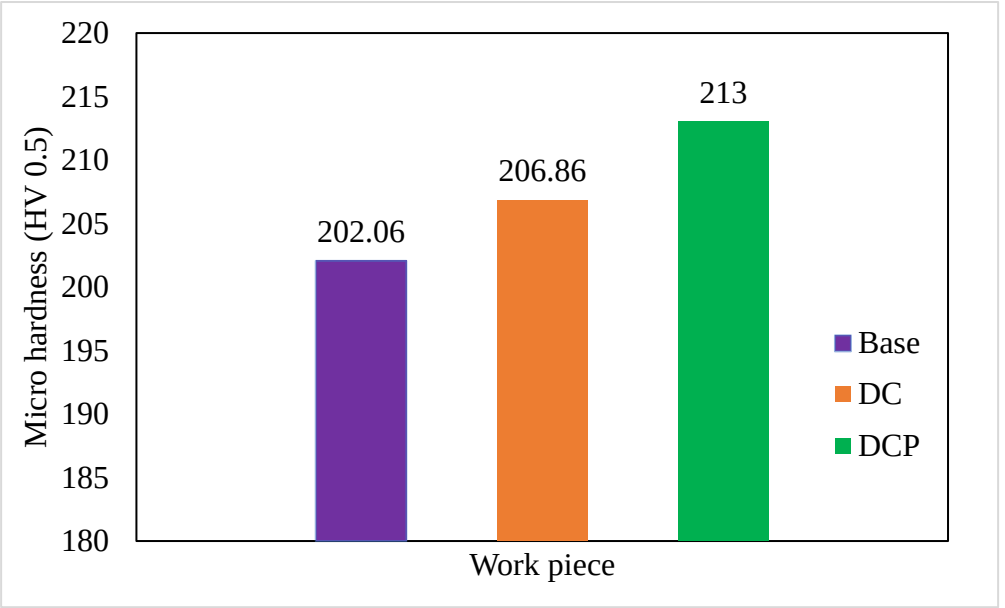

Figure 5 Microhardness measurement

3.4 Hot corrosion study

The Base and build walls are tested at about 900°C high for fifty cycles to identify their capability at elevated temperatures. Unlike typical corrosion, hot corrosion always takes place with two steps. Once the samples were exposed to the salt medium at high temperatures, the combination of the salts started attacking the samples (Base, DC, and DCP walls).

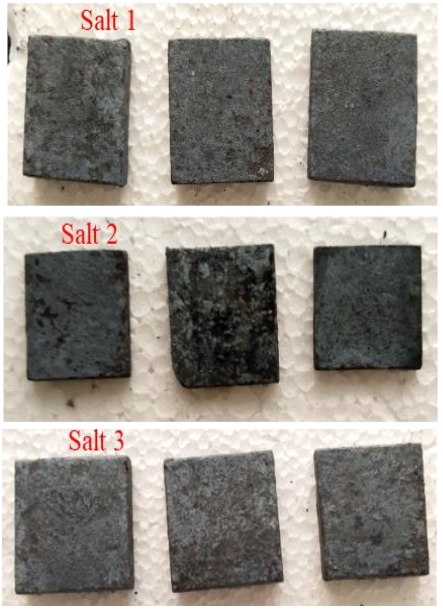

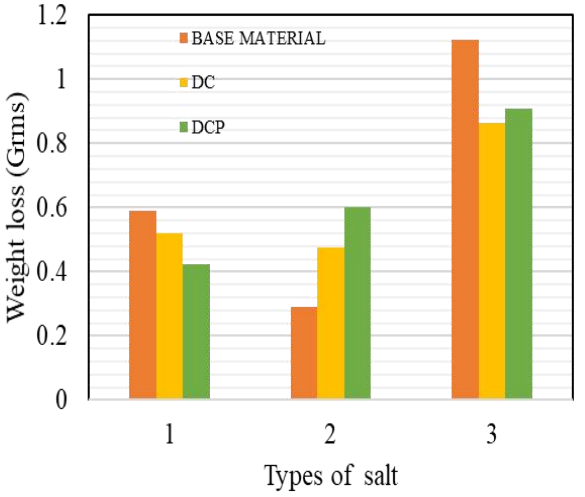

Figure 6 Effect of various slats on weight loss after 50 cycles for the Base and walls

To maintain stability against the salt attack, the alloying elements in the steel 316L, such as Nickel, Chromium started producing the oxide layers over the surfaces [19-20]. Based on this, Figure 6 shows the results of the hot corrosion tested with (salt mixture 1 (70% Na2SO4+ 25% NaCl +5% V2O5), salt mixture 2 (75% Na2SO4 + 23% NaCl + 3% V2O5), and salt mixture 3 (75% Na2SO4 + 25% NaCl)). Base metal (0.58992 Gram) and DC (0.518157 Gram) show more weight loss than the DCP wall for salt 1. Next, except base metal, both DC (0.4769165 Gram) and DCP (0.60225 Gram) walls show maximum weight loss for the salt 2. 75% Na2SO4 + 25% NaCl leads to ultimate weight loss (1.12303 Gram) to base metal for the salt mixture combination. But the walls are having less weight loss as compared to its Base.

4 CONCLUSION

- The walls are built with two different modes of MIG welding equipment. Based on the studies, the parameters of DC and DCP are revealed for fabricating the defect-free walls. For the 250 mm/min speed, the welding current as 120A for DC and 90 (I avg) for DCP are selected. The beads came with smooth profiles without delamination, voids, and cracks.
- The average microhardness measurement revealed that increasing the hardness by four counts for DC and eleven counts for DCP as compared with the base metal of stainless steel 316L.
- The tensile test showed that base metal has the highest strength of 661MPa. But the walls have more elongation as compared to base metal. The DCP mode has reached the maximum strain of 55% with intermediate properties between the base and DC mode walls.
- The hot corrosion studies identified that the combination of 75% Na2SO4 + 25% NaCl (salt mixture 3) is complicated to face by the stainless steel 316L base and walls. For the salt mixture 2 (75% Na2SO4 + 23% NaCl + 3% V2O5), the attacks were not much, and the weight loss was minimal at the temperature of 900°C. For all salt mixture conditions, DC walls have the average weight loss.

ACKNOWLEDGEMENTS

The authors are thankful to file no SERB/2019/0000676 and National Institute of Technology -Patna in association with TEQIP-III for providing the research support regarding equipment, materials, and human resources (Mr. Hemant Priyadarshi - JRF). The authors also thank the procurement head (Prof. Prakash Chandra) and their teams (NIT-Patna) for their extreme support. The authors loved acknowledging the material characterization laboratory from the Department of Mechanical Engineering, National Institute of Technology Puducherry (Karaikal).

References

1. Baddoo, N. R. (2008). Stainless steel in construction: A review of research, applications, challenges and opportunities. Journal of constructional steel research, 64(11), 1199-1206.
2. Di Schino, A. (2020). Manufacturing and applications of stainless steels. Metals, 10(3), 327.
3. Rane, K., Cataldo, S., Parenti, P., Sbaglia, L., Mussi, V., Annoni, M., ... & Strano, M. (2018, May). Rapid production of hollow SS316 profiles by extrusion based additive manufacturing. In AIP Conference Proceedings (Vol. 1960, No. 1). AIP Publishing.
4. Zhong, Y., Rännar, L. E., Liu, L., Koptyug, A., Wikman, S., Olsen, J., ... & Shen, Z. (2017). Additive manufacturing of 316L stainless steel by electron beam melting for nuclear fusion applications. Journal of nuclear materials, 486, 234-245.
5. Balit, Y., Charkaluk, E., Constantinescu, A., & Durbecq, S. (2019). Microstructure and process parameters for directed energy deposition additive manufacturing. The Romanian Journal of Technical Sciences. Applied Mechanics., 64(3), 175-188.
6. Karpagaraj, A., Baskaran, S., Arunnellaiappan, T., & Kumar, N. R. (2020, July). A review on the suitability of wire arc additive manufacturing (WAAM) for stainless steel 316. In AIP Conference Proceedings (Vol. 2247, No. 1). AIP Publishing.
7. Rodrigues, T. A., Escobar, J. D., Shen, J., Duarte, V. R., Ribamar, G. G., Avila, J. A., ... & Oliveira, J. P. (2021). Effect of heat treatments on 316 stainless steel parts fabricated by wire and arc additive manufacturing: Microstructure and synchrotron X-ray diffraction analysis. Additive Manufacturing, 48,102428.
8. Chen, X., Li, J., Cheng, X., Wang, H., & Huang, Z. (2018). Effect of heat treatment on microstructure, mechanical and corrosion properties of austenitic stainless steel 316L using arc additive manufacturing. Materials Science and Engineering: A, 715, 307-314.
9. Wang, L., Xue, J., & Wang, Q. (2019). Correlation between arc mode, microstructure, and mechanical properties during wire arc additive manufacturing of 316L stainless steel. Materials Science and Engineering: A, 751, 183-190.
10. Chen, J., Wei, H., Bao, K., Zhang, X., Cao, Y., Peng, Y., ... & Wang, K. (2021). Dynamic mechanical properties of 316L stainless steel fabricated by an additive manufacturing process. Journal of Materials Research and Technology, 11, 170-179.
11. Vishnukumar, M., Muthupandi, V., & Jerome, S. (2022). Effect of post-heat treatment on the mechanical and corrosion behaviour of SS316L fabricated by wire arc additive manufacturing. Materials Letters, 307, 131015.
12. Cunningham, C. R., Wang, J., Dhokia, V., Shrokani, A., & Newman, S. T. (2019). Characterisation of Austenitic 316 LSi Stainless Steel Produced by Wire Arc Additive Manufacturing with Interlayer Cooling. In 2019 International Solid Freeform Fabrication Symposium. University of Texas at Austin.
13. AbouelNour, Y., & Gupta, N. (2022). In-situ monitoring of sub-surface and internal defects in additive manufacturing: A review. Materials & Design, 111063.
14. Tomar, B., Shiva, S., & Nath, T. (2022). A review on wire arc additive manufacturing: Processing parameters, defects, quality improvement and recent advances. Materials Today Communications, 31,103739.
15. Wu, B., Pan, Z., Ding, D., Cuiuri, D., Li, H., Xu, J., & Norrish, J. (2018). A review of the wire arc additive manufacturing of metals: properties, defects and quality improvement. Journal of manufacturing processes, 35, 127-139.
16. Vemanaboina, H., Babu, M. M., Prerana, I. C., Gundabattini, E., Yelamasetti, B., Saxena, K. K., ... & Agrawal, M. K. (2023). Evaluation of residual stresses in CO2 laser beam welding of SS316L weldments using FEA. Materials Research Express, 10(1), 016509.
17. Reddy, K. S., Vemanaboina, H., Naidu, B., Yelamasetti, B., Bridjesh, P., & Shelare, S. D. (2023). Minimizing distortion in multi-pass GTAW welding of SS316L structures: a Taguchi approach. International Journal on Interactive Design and Manufacturing (IJIDeM), 1-8.

18. Samanta, S. K., Mitra, S. K., & Pal, T. K. (2008). Microstructure and oxidation characteristics of laser and GTAW weldments in austenitic stainless steels. Journal of materials engineering and performance, 17, 908-914.
19. Meng, J. S., Chen, M. X., Shi, X. P., & Qiang, M. A. (2021). Effect of Co on oxidation and hot corrosion behavior of two nickel-based superalloys under Na2SO4–NaCl at 900° C. Transactions of Nonferrous Metals Society of China, 31(8), 2402-2414.
20. Sundaresan, C., Rajasekaran, B., Varalakshmi, S., Santhy, K., Rao, D. S., & Sivakumar, G. (2021).Comparative hot corrosion performance of APS and Detonation sprayed CoCrAlY, NiCoCrAlY and NiCr coatings on T91 boiler steel. Corrosion Science, 189, 109556.